

REVIEW ARTICLE



The evolution of pleomorphic xanthoastrocytoma: from genesis to molecular alterations and mimics

Swati Mahajan¹, Iman Dandapath¹, Ajay Garg², Mehar C. Sharma¹, Vaishali Suri¹✉ and Chitra Sarkar¹✉

© The Author(s), under exclusive licence to United States and Canadian Academy of Pathology 2022

Pleomorphic xanthoastrocytomas (PXAs) are rare tumors accounting for less than 1% of astrocytomas. They commonly occur in young patients and have relatively favorable prognosis. However, they are well known to have heterogenous morphology and biological behavior with the potential to recur and disseminate throughout the central nervous system, especially their anaplastic counterparts. Recent advances in the molecular characterization have discovered *BRAFp.V600E* mutations in conjunction with *CDKN2A/B* deletions and *TERTp* mutations to be the most frequent alterations in PXAs. These tumors can present a diagnostic challenge as they share overlapping histopathological, genomic as well as methylation profile with various other tumor types, particularly epithelioid glioblastomas (eGBs). This review provides the spectrum of evolution of PXAs from their genesis to recent molecular insights and attempts to review pathogenesis and relationship to other tumors that they mimic especially eGB. It is postulated based on evidence from literature that PXA and eGB are possibly related and not distinct entities, being two ends of a continuous spectrum of malignant progression (grade 2–grade 4) with anaplastic PXA (grade 3) lying in between. Future WHO classifications will have to possibly redefine these tumors using more confirmatory data from larger studies.

Laboratory Investigation (2022) 102:670–681; <https://doi.org/10.1038/s41374-021-00708-0>

INTRODUCTION

Kepes et al. first introduced the term “pleomorphic xanthoastrocytoma (PXA)” to describe a distinctive type of “meningocerebral glioma occurring mainly in young subjects and associated with a relatively favorable prognosis”. These tumors were histologically characterized by pleomorphism, mitosis, presence of spindle and multinucleated giant cells (GCs), many with large amounts of lipid in their cytoplasm and rich pericellular reticulin network, thus simulating a mesenchymal tumor¹. In view of the above features, these tumors had been earlier misdiagnosed as meningocerebral fibrous xanthomas. Kepes et al. however recognized these as tumors of astrocytic nature based upon their immunopositivity for glial fibrillary acidic protein (GFAP). They postulated subpial astrocytes to be their cell of origin based on ultrastructural features of presence of basal laminae surrounding tumor cells. All the 12 cases first described by Kepes et al. had a relatively favorable prognosis with long survival times up to 25 years¹. The anaplastic nature of PXAs was first recognized by Weldon-Linne et al. in 1983 who reported the first case of recurrent PXA with malignant transformation in a 32-year-old man with rapid fatal outcome². Later Iwaki et al. reported a case of PXA, which showed anaplastic evolution 6 months postoperatively³. Similarly, Kepes et al. in 1989 reported three cases of postsurgical recurrence of PXA with progression into a more malignant type, either an anaplastic astrocytoma or a glioblastoma (GB). The time required for such transformations varied from 7 months to 15 years⁴.

PXA was included as a distinct entity in the World Health Organization (WHO) classification of central nervous system (CNS)

tumors in 1993 as a grade II neoplasm and was defined as “An astrocytic neoplasm with a relatively favorable prognosis, typically encountered in children and young adults, with superficial location in the cerebral hemispheres, involvement of the meninges, and a pleomorphic histological appearance that includes lipidized GFAP-expressing tumor cells surrounded by a reticulin network”⁵.

Though the definition and grading remained the same in the 2000 as well as 2007 WHO classifications, the presence of eosinophilic granular bodies (EGB) was added as a characteristic feature of PXA in the definition^{6,7}. Further, in both 2000 and 2007 WHO classifications, PXA with 5 or more mitosis/10 high-power field (HPF) and/or with areas of necrosis was designated as “PXA with anaplastic features” owing to their relatively worse prognosis. The use of the term “anaplastic PXA (A-PXA)” grade III was however not recommended^{6,7}.

Over the years, substantive experience accumulated through original studies and reviews on PXA and A-PXA and it became clear that A-PXAs acquire features of a more aggressive astrocytic neoplasm that include increased proliferation, necrosis, microvascular proliferation, loss of pericellular reticulin, and increased infiltrative growth^{8–10}. Therefore, in 2016 WHO classification, PXA was redefined as “An astrocytic glioma with large pleomorphic and frequently multinucleated cells, spindle and lipidized cells, a dense pericellular reticulin network, and numerous eosinophilic granular bodies”. In addition the term “A-PXA” was introduced as a separate entity (grade III tumor) and was defined as “A pleomorphic xanthoastrocytoma with ≥ 5 mitosis/10 HPF”¹¹. Further, with advances in molecular profiling it became clear that combined

¹Department of Pathology, All India Institute of Medical Sciences, New Delhi, India. ²Department of Neuroimaging & Interventional Neuroradiology, All India Institute of Medical Sciences, New Delhi, India. ✉email: surivaishali@yahoo.co.in; sarkar.chitra@gmail.com

Received: 1 August 2021 Revised: 15 November 2021 Accepted: 18 November 2021

Published online: 14 January 2022

BRAFp.V600E mutation and homozygous deletion of *CDKN2A/B* are the characteristic molecular alterations that occur in PXA and hence their presence in the absence of IDH mutation strongly supports the diagnosis^{12–17}.

In the upcoming 2021 WHO classification, in order to bring uniformity in the classification and grading of CNS tumors with tumors of all other organ systems, the term “anaplastic” has been removed and the use of Arabic numerals has been introduced instead of Roman numerals. The danger of using Roman numerals is that the typographical mistakes can occur between a grade “II” and a grade “III” tumor or a grade “III” tumor and a grade “IV” tumor, which could have serious clinical implications. Therefore, PXA is now designated as either CNS grade 2 or grade 3, thus obviating the term “A-PXA.” Definition of PXA remains the same as of 2016, and additionally the presence of molecular alterations viz. *BRAFp.V600E* (or other *MAP kinase (MAPK)* pathway gene alterations) and homozygous *CDKN2A/CDKN2B* deletion have been added to it¹⁸.

Epidemiology

PXAs constitute <0.3% of primary CNS tumors and <1% of all astrocytic tumors with an annual incidence of <0.7 cases per 100,000 population^{17,18}. In Surveillance, Epidemiology, and End Results, a total of 346 PXA grade II and 62 A-PXA have been reported between 2000 and 2016 in the USA¹⁹. In the Central Brain Tumor Registry of the United States, PXA is still classified under the umbrella term “unique astrocytoma variants”²⁰. Very little data regarding prevalence of A-PXA are available to date. One series reported anaplasia in 31% (23/74) of cases at first diagnosis²¹. Giannini et al. reported increased mitotic activity (≥ 5 mitosis/10 HPF) in 18% and necrosis in 11% of their 71 cases at diagnosis¹⁰.

Location

PXAs occur most commonly in the superficial cortex of the cerebral hemispheres, often involving the overlying leptomeninges^{6,22,23}. Temporal lobe is the most frequent site; rarely they have been reported to occur in the cerebellum, spinal cord, thalamus, orbit, retina, pineal gland and sella turcica^{18,24–26}. One study has also reported multicentric occurrence of PXA presenting with several noncontiguous lesions at time of diagnosis²⁷. These tumors also have the potential to spread via the cerebrospinal fluid (CSF), more commonly seen during the recurrence or malignant transformation setting^{8,28,29}.

Clinical features

PXAs are most commonly diagnosed in the first and second decade of life with mean age at diagnosis being 26.3 years (median 20.5). But cases as young as 2 years and up to 8th decade have been reported^{10,18,30}. There appears to be no gender predilection⁷. Owing to the superficial cerebral location, most common presenting symptom is a long history of seizures, spanning months to years prior to radiographic diagnosis¹⁰. PXAs at other sites generally have slow but progressive symptoms of an expanding mass related to their location. Only a limited number of patients present with CSF disseminated disease at their initial diagnosis^{8,28,29}.

Imaging

PXAs most commonly occur as supratentorial, superficial cortically based hemispheric masses with leptomeningeal contact^{10,31–33}. Three radiological patterns have been identified (a) cystic lesion with an enhancing mural nodule that abuts or is attached to leptomeninges (most common)^{1,10}, (b) solid mass with cystic

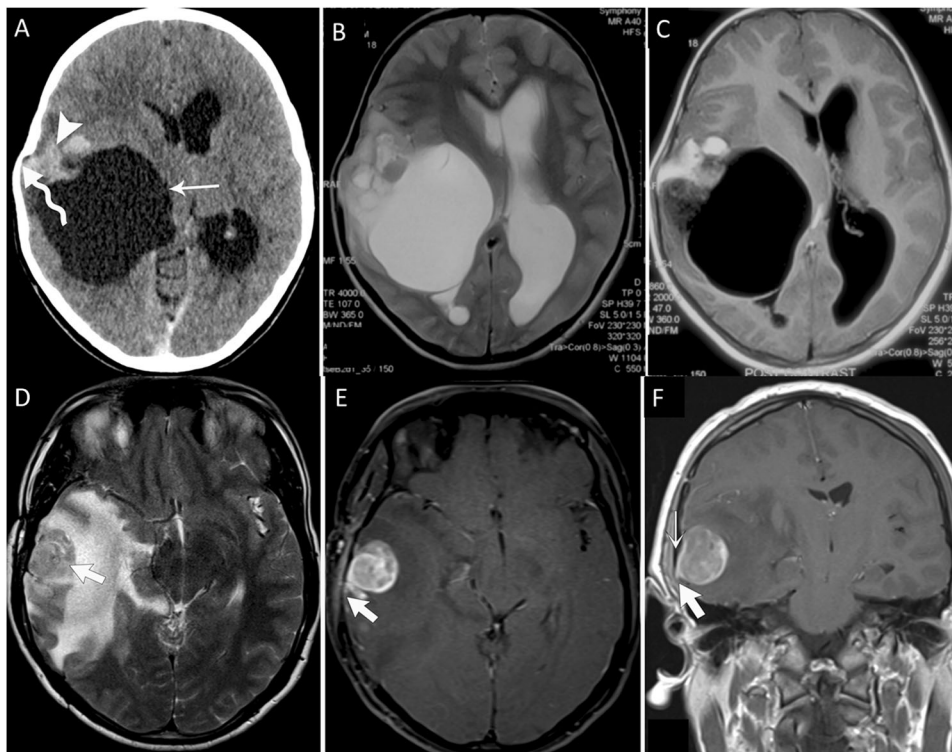


Fig. 1 Imaging characteristics of a case of pleomorphic xanthoastrocytoma (PXA) and anaplastic-PXA. **A–C** A case of pleomorphic xanthoastrocytoma. An axial CECT image (**A**) shows a large cystic lesion (thin arrow) with intensely enhancing mural nodule (arrowhead) in right parietal lobe causing scalloping of adjacent parietal bone (wavy arrow) and mass-effect on ipsilateral lateral ventricle and midline shift. On MRI, the cyst is hyperintense on T2-WI (**B**) and hypointense in postgadolinium T1-WI (**C**), while solid mural nodule is iso-hyperintense on T2-WI (**B**) and enhancing in postgadolinium T1-WI (**C**). **D, E** A case of anaplastic pleomorphic xanthoastrocytoma. MRI shows a cortical based iso-hyperintense mass lesion in T2-WI (**D**) in right temporal lobe with extensive perilesional edema. The mass is abutting the pial surface and shows intense contrast enhancement (**E, F**) along with focal leptomeningeal enhancement (arrow in **E**) in postgadolinium T1-WI (**E, F**).

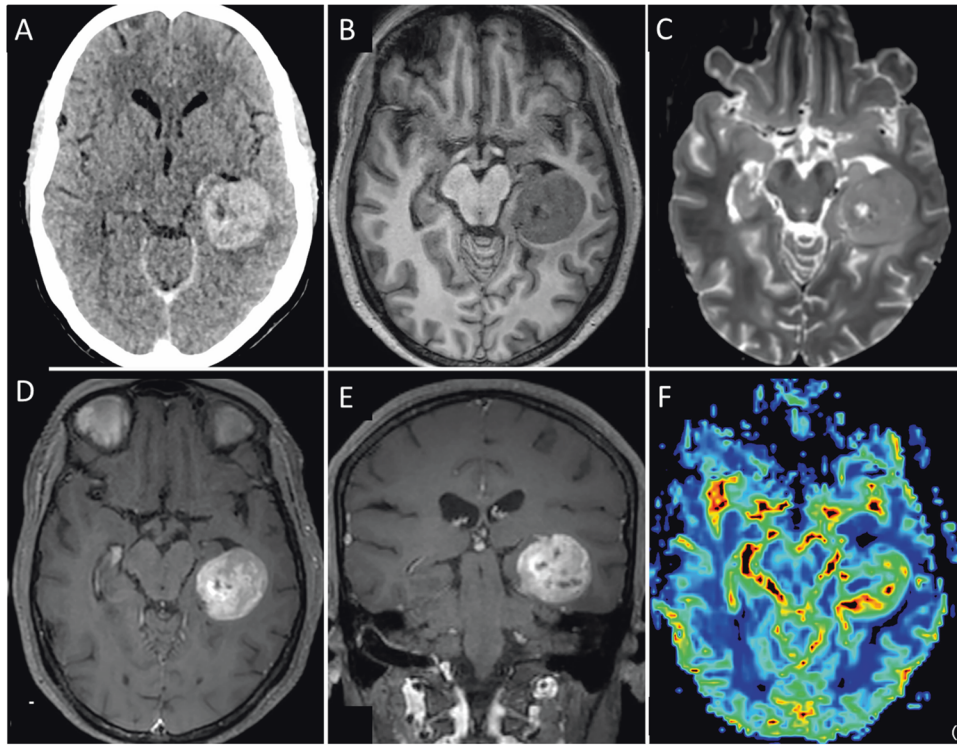


Fig. 2 Imaging characteristics of a case of epitheloid glioblastoma. CECT image (A) shows an intensely enhancing mass lesion with few cystic components in left temporal lobe. On MRI, lesion is isointense on T1- (B) and T2-WI (C) with minimal perilesional edema. On postcontrast axial (D) and coronal (E) T1-WIs, lesion appears to be cortical based and shows vivid enhancement with few nonenhancing cystic components. Dynamic susceptibility perfusion imaging (F) shows significant raised perfusion in the lesion suggesting highly malignant lesion.

degeneration reported in 30% cases³¹ and (c) unilocular or multicystic lesion^{1,10,32}. The tumor margins can be well or poorly defined with a variable amount of surrounding brain edema.

On contrast-enhanced computed tomography (CECT), the tumor appearance is variable, with cystic components usually appearing hypodense and solid components appearing hypo to isodense and rarely hyperdense (Fig. 1A). The solid component and the wall of the cyst usually show moderate to intense enhancement. Focal calcification may also be seen in the solid component. There may be scalloping of the overlying skull^{31,32}.

On magnetic resonance imaging (MRI), cystic component is hypointense on T1- and hyperintense on T2-weighted images (WIs) whereas the solid component including mural nodules or thick cyst walls of tumors are hypointense or isointense on T1- and slightly hyperintense on T2-WI. Marked enhancement of the solid component and peripheral rim enhancement of the cyst is seen on T1-WIs with gadolinium enhancement (Fig. 1B, C). Leptomeningeal enhancement is reported in $\approx 14\%$ of cases, which contrasts with the fact that leptomeningeal contact is evident in 92% of the lesions^{31,33}.

PXA is hypovascular on angiography³⁴. On fluorodeoxy glucose positron emission tomography, it shows high glucose metabolism and hypoperfusion on SPECT perfusion scans³⁵. Compared to PXA, A-PXAs typically are larger lesions with more heterogeneous-appearing masses. These tumors are more likely to have leptomeningeal spread and have increased perfusion parameters (Fig. 1D–F)^{8,34}.

Radiologically PXA should be considered in the differential diagnosis of peripheral cystic lesions with an enhancing mural nodule and also any enhancing lesion that shows extensive involvement of the leptomeninges in a young patient. It includes ganglioglioma (GG), pilocytic astrocytoma (PA), dysembryoplastic neuroepithelial tumor (DNET), and meningioma. Compared to PXA, GG usually show extensive calcification along with nil to mild

peritumoral edema. PA often occurs in the area of optic chiasma, cerebellum, fourth ventricle and brainstem, whereas PXA mostly occurs in the cerebral hemispheres. Cortical dysplasia near the tumor and nonenhancement on contrast medium is useful in differentiating DNET from PXA^{31,33,34}. Compared to PXA, meningiomas more commonly present with leptomeningeal enhancement also known as a “dural tail” sign (60%) and rarely with cystic degeneration. Epitheloid GB (eGB) characteristically presents as a Gd-enhancing solid mass, occasionally with cysts^{31,32}. The diffusion may be restricted (Fig. 2). These tumors are prone to hemorrhage and often spread through the leptomeninges. These tumors are indistinguishable from GB on imaging, with enhancement, necrosis and diffusion restriction present in the vast majority of tumors^{31,32}.

Pathogenesis

Kepes et al. proposed that PXAs originate from subpial astrocytes thus explaining the superficial cortical location of these tumors. This hypothesis was also supported by the ultrastructural features shared by subpial astrocytes and PXA tumor cells³⁶.

Macroscopy

PXAs usually appear as well circumscribed, firm to partially cystic, superficial cortical masses, commonly involving the overlying leptomeninges¹⁰. The superficial circumscription is however deceptive, since the deeper portions often exhibit underlying parenchymal infiltration. The solid parts of the tumor generally appear as ivory-colored or gray white firm avascular masses without evidence of necrosis. Some tumors may appear yellowish in color due to extensive lipidization of tumor cells. The cystic part is either uni- or multiloculated and may contain clear, yellow, or xanthochromic fluid, and is usually located deep to the solid part. Invasion of the dura, predominant exophytic growth, and leptomeningeal dissemination are however rare^{10,18,37}.

Histopathology

PXA. A very important hallmark of these neoplasms is the superficial location associated with leptomeningeal involvement. This can be identified under the microscope by the identification of (a) leptomeningeal large caliber muscularised arteries embedded within the tumor and (b) tumor cells surrounding cortical vessels in the perivascular Virchow Robin spaces. In addition to the discrete solid superficial located component, many tumors show an element of invasion into the underlying brain parenchyma³⁸. The cells within the infiltrative component are often less pleomorphic than in the superficial part, thus resembling diffuse astrocytoma both cytologically and architecturally³⁷.

Histologically, PXAs are moderately to highly cellular tumors composed of pleomorphic cells arranged in fascicular or storiform pattern, giving a mesenchymal appearance to the tumor. The tumor cells are either spindle shaped with elongated nuclei or large polygonal epithelioid cells with single to multilobulated nuclei or multiple nuclei (bizarre multinucleate GCs). The cytoplasm of the tumor cells is either eosinophilic or foamy and vacuolated due to accumulation of lipid droplets (Fig. 3A, C). These xanthomatous cells with foamy cytoplasm are diagnostically helpful, but were seen in ~25–83% of cases in different series^{1,10,28,29}. One of the most characteristic features of PXAs is deposition of patchy to widespread intercellular reticulin network, either individually around tumor cells, or more commonly surrounding small groups of tumor cells (as cell clusters) (Fig. 3E). Intranuclear pseudo-inclusions and EGBs are almost constant findings³⁰. Cells with intracytoplasmic eosinophilic hyaline/protein droplets are commonly seen. Rosenthal fibers (RFs) may also be observed particularly at the edges of the tumor¹⁰. Focal perivascular or intratumoral collections of mature lymphocytes with occasional plasma cells are a frequent finding¹⁰. Unique histopathology with abundant clear cells and focal papillary appearance or rare presence of pigment containing cells has also been reported^{39,40}.

Necrosis is usually absent and mitoses are low or absent (<5 mitosis/10 HPF or 2.5 mitosis/mm² equating 1 HPF to 0.23 mm² in area or 0.54 mm in diameter). MIB-1 labeling index is generally <1%. The relative lack of mitosis in the setting of marked pleomorphism is a characteristic feature in the diagnosis of PXA.

It must be emphasized that the histological features of PXA are variable and neither all of the typical characteristics are present simultaneously nor in all cases which may well cause a diagnostic challenge, particularly in the discrimination of PXAs from the mimics. In the series of Giannini et al. and Furutu et al., EGBs were seen in 81–83%, RFs in 27%, intranuclear inclusion in 87%, xanthomatous change in 66–83%, lymphocytic infiltrate in 83–100% and calcification in 18% PXA cases^{10,41}.

A-PXA. A-PXA may manifest de novo or at recurrence. A-PXA is primarily defined by the presence of high mitotic activity, usually 2.5 or more mitosis/mm² (equating 5 or more mitoses/10 HPF in which 1 HPF equals 0.23 mm² in area and 0.54 mm in diameter). Necrosis is usually seen in tumors with high mitotic activity, however its significance in isolation is indeterminate currently¹⁸. The mean KI-67 (MIB-1) labeling index reported is around 15%. A-PXA shares similar morphological features with PXA but may harbor areas demonstrating proliferation of monomorphic tumor cells instead of pleomorphic, loss of pericellular reticulin and tumor cell infiltration with entrapped neuropil (Fig. 3B, D, F)^{4,8,11}. EGBs can be seen in 80–100%, intranuclear inclusion in 87%, xanthomatous change in 73%, calcification in 20% and necrosis in 13–80% of A-PXA cases^{42,43}. Additional histological patterns like distinct areas of high-grade small cell and fibrillary or epithelioid cell morphology have also been reported in a subset of A-PXA¹⁷. Extensive presence of epithelioid cells (comprising >30% of tumor) was noted in 33% cases of A-PXA cases in a study by Wang et al.⁴³.

Immunohistochemistry

Immunohistochemical studies demonstrate diffuse and strong positivity with the antibodies against GFAP and S100 protein supporting a glial, and more specifically an astrocytic, cell of origin^{10,11,44}. Olig-2 and SOX2 immunoreactivity is also commonly seen. Many PXAs demonstrate focal positivity with the antibodies against neuronal markers including synaptophysin, neurofilament, class 3b-tubulin and MAP2⁶. The hematopoietic progenitor/vascular endothelial cell-associated antigen CD34 is expressed in tumor cells in up to 50% of cases⁴⁴. The immunohistochemical profile aids in distinguishing this tumor from mesenchymal or meningothelial neoplasms. The p53 mutant protein expression is variable across reported cases, with most tumors being entirely negative⁴⁵. The immunohistochemical profile of PXA and A-PXA are similar.

Molecular genetic landscape of PXA and A-PXA

Advances in molecular characterization of CNS neoplasms have made significant contributions to our current understanding of PXA as a unique neoplasm that is often genotypically distinct from diffuse infiltrating gliomas. The earliest analysis of PXA was related to TP53, revealing mutations in 6% (6/125) of cases analyzed in three independent studies, with no correlation to anaplastic features^{45–47}. Genetic alterations typical of infiltrating gliomas, such as amplifications of the *EGFR*, *MDM2* or *CDK4* loci were found to be distinctly rare or absent in most PXA⁴⁷.

Over recent years, genomic analyses has made significant contributions to our current understanding of molecular alterations in PXA and have identified *MAPK* pathway alterations and *CDKN2A/B* homozygous deletions to be the most common and consistent genetic abnormality in PXAs^{12,13}. Various common alterations reported in PXA are discussed below (Fig. 4).

CDKN2A/B homozygous deletion. Comparative genomic hybridization analysis of 50 PXA by Weber et al. first identified loss of chromosome 9 as the most common chromosomal alteration in these tumors. Furthermore, 60% of PXAs were found to carry homozygous deletions of 9p21.3 involving the *CDKN2A/p14ARF* and *CDKN2B* tumor-suppressor gene loci¹⁴. Later several independent studies identified *CDKN2A/B* deletion to be a common genomic alteration in PXA with frequency ranging from 60% to >85%, irrespective of tumor grade^{48–51}. Vaubel et al. detected *CDKN2A/B* loss in 83% PXA and 93% A-PXA, respectively¹⁷. Homozygous/biallelic deletion of the *CDKN2A* locus at 9p21 was also identified in 95% (18/19) of PXA/A-PXA cases in a study by Phillips et al.⁵⁰. However, Zou et al. in their series reported its frequency to be far lower (8%, 1/13 PXA) as compared to other studies⁵². The difference might partly reflect variability across patient cohort, histological diversity of PXA as well as technical differences in the methods used to detect *CDKN2A/B* deletion in various studies.

BRAFp.V600E mutation. By far the most frequent *MAPK* pathway alteration reported in PXA is *BRAFp.V600E* mutation, which has been identified in 38–80% of PXA by various studies^{12,13,17,21,49,50}. Zou et al. detected *BRAF* mutation in only 38% of patients⁵². However, Vaubel et al. reported *BRAFp.V600E* in 79.2% PXA (42/53) and 64.3% A-PXA (9/14)⁴⁸. Similarly, Ida et al. found *BRAFp.V600E* mutation in 73.2% (30/51) PXA and 47.4% (9/23) A-PXA cases²¹. Further, they demonstrated that *BRAF* mutation divides these tumors into two clinically relevant subgroups, with regard to both natural history and response to therapy. Patients with *BRAFp.V600E*-mutant tumors had significantly longer overall survival (OS) as compared to those with *BRAFp.V600E* wild-type (wt) tumors ($P = 0.02$). The presence of *BRAF* mutations has also emerged as a potential target in PXA, as *BRAFp.V600E* can be targeted therapeutically by small molecule inhibitors of both *RAF* (e.g., vemurafenib) and *MEK* (e.g., trametinib)²¹. Though currently very

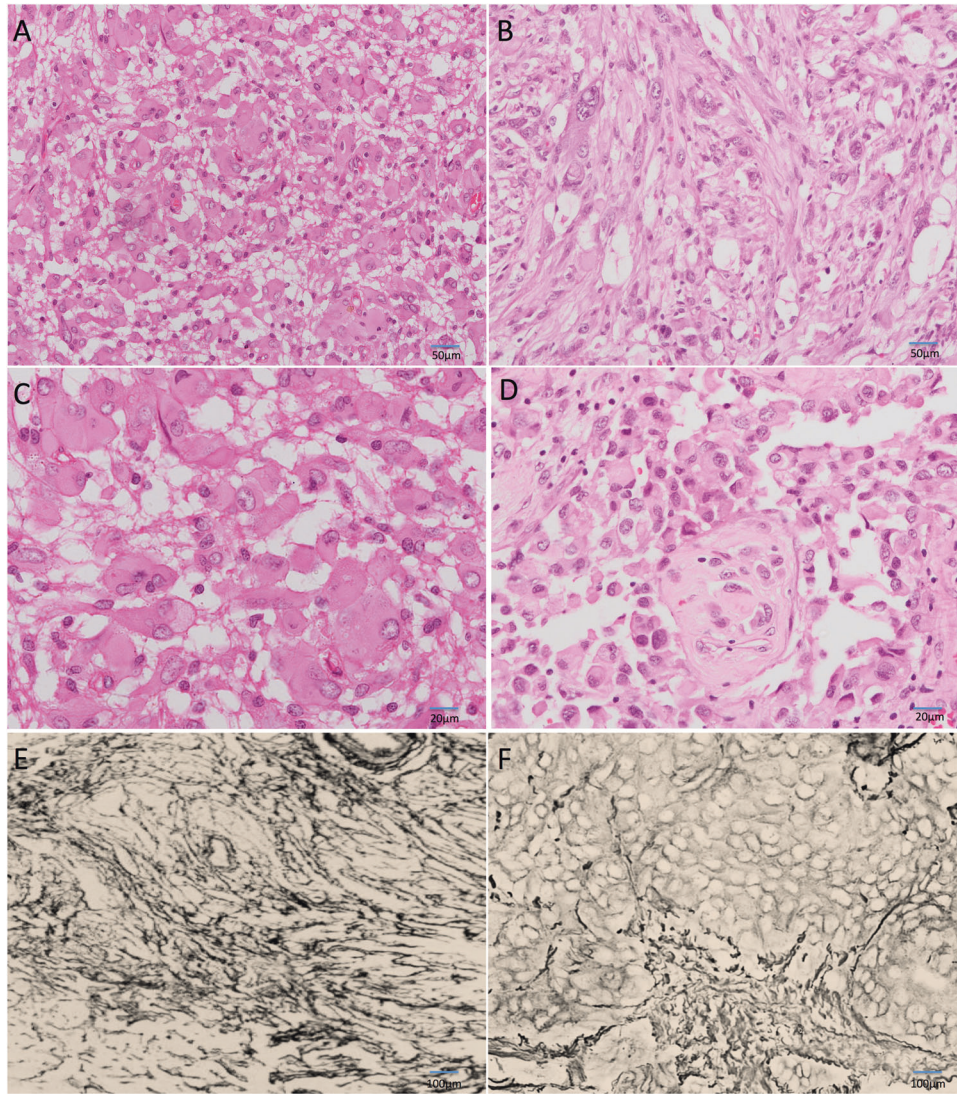


Fig. 3 Histologic features of pleomorphic xanthoastrocytoma (PXA) and anaplastic PXA. Characteristic features of PXA, WHO grade II (left column), include pleomorphic, spindled to bizarre looking multinucleated tumor cells with abundant eosinophilic cytoplasm and xanthomatous cells (A, C). In addition it shows EGBs, pericellular reticulin (E) and relative lack of mitotic activity. Anaplastic PXA, WHO grade III (right column), shares morphological features with PXA (B) but in addition it may exhibit mitotic activity, palisading necrosis and/or focal solid area with numerous epithelioid cells (D), however it shows relative paucity of EGBs, xanthomatous cells and pericellular reticulin network (F).

limited data are available on such therapeutic strategies for PXAs, this avenue is expected to be actively explored in the near future. In addition across all pediatric gliomas, the combination of *BRAF* mutation and *CDKN2A/B* homozygous deletion is common in low-grade tumors that transform to high grade and is associated with poor response to current adjuvant therapies^{15,16}.

TERT promoter mutation. After *BRAFp.V600E* mutation and *CDKN2A* homozygous deletion, the most common alteration identified in PXA is the alteration of the *TERT* gene. *TERT* promoter (*TERTp*) mutation is reported to be more frequent in A-PXA as compared to PXA. Vaubel et al. and Koelshe et al. identified *TERTp* mutation in only 2% (1/21) and 4% (1/25) of PXA while the frequency was 14.3% (2/14) and 23% (3/23) in A-PXA^{48,53}. Kurshonov et al. however observed these mutations in 19% of PXA and 36% of A-PXA⁵¹. Phillips et al. identified *TERT* gene alterations in 47% (7/15) of A-PXA cases. Two tumors contained amplification of the *TERT* gene and five tumors harbored a hotspot mutation in the promoter region of *TERT*⁵⁰. They also suggested that the *TERT* promoter alterations are likely

to contribute to anaplastic progression in PXA as in one case they noted *TERTp* mutation accompanied anaplastic progression in matched tumor pair. Thus, overall studies suggest that *TERT* alterations are associated with recurrence, anaplastic transformation and poor outcome.

Other alterations of MAPK pathway. Other *MAPK* alterations identified in a smaller fraction of PXA negative for *BRAFp.V600E* mutation include *BRAF* insertion/deletion mutations⁵⁴, fusions involving *BRAF* or *RAF1*⁵⁵, *ETV6-NTRK3* fusion⁵⁶ and mutation of *TSC2* and *NF1*⁵⁷. Fusions of *NRF1-BRAF* and *ATG7-RAF1* have also been reported in A-PXA using a targeted next-generation sequencing panel⁵⁸.

Other chromosomal gains/losses. PXAs show frequent additional copy number variants (CNVs), predominantly involving whole chromosome or chromosomal arm gains and losses. Recurrent alterations reported across multiple studies include loss -9 or -9p, -22 and -13; recurrent gains include +7, +2, +5, +12, +20, +15 and +21^{14,17,50}. Vaubel et al. reported loss/copy neutral loss

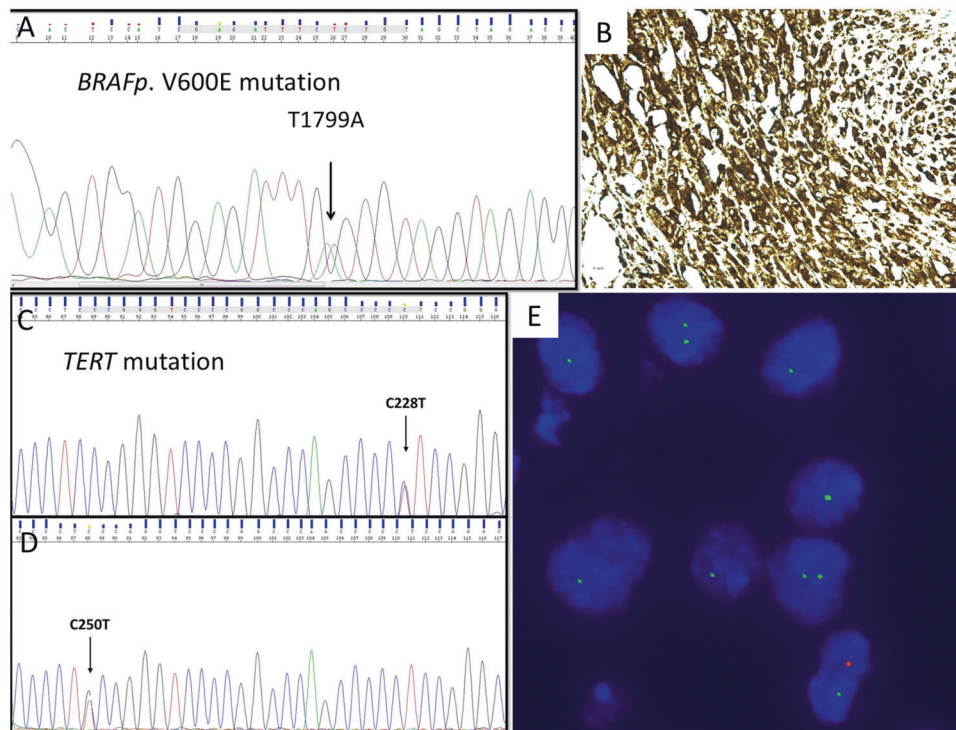


Fig. 4 Common molecular alteration seen in pleomorphic xanthoastrocytoma and anaplastic PXA. Mutation profiling of PXA and A-PXA cases can reveal *BRAFp.V600E* mutations (**A**, using Sanger sequencing or **B**, immunohistochemistry), *TERT* promoter mutations (**C**, **D**, using Sanger sequencing) and *CDKN2A/B* homozygous deletions (**E**, using fluorescent in situ hybridization assay). For *CDKN2A* assay locus-specific probes paired with centromere probes for chromosomes 9 (Vysis LSI *CDKN2A* Spectrum Orange/CEP9 Spectrum green probes, Downers Grove, IL) were used. Homozygous deletion of the *CDKN2A* was considered when loss of both orange signals in each nucleus was seen in a minimum of 20% nuclei.

of heterozygosity of chromosomes 14 and 22 to be significantly associated with anaplastic grade and gains of +12 and +21 to be significantly more common in *BRAF* mutant tumors. Further, six out of the ten cases with matched primary/recurrent tumors or matched areas of low-/high-grade morphology in their study showed numerous additional CNVs in the high-grade areas and recurrent tumors¹⁷. Phillips et al. similarly reported an increase in CNVs over time in three out of four matched tumor pairs of primary and corresponding recurrent tumor thus indicating that PXA undergo a period of chromosomal instability during anaplastic progression during which it acquires numerous chromosomal gains and losses⁵¹. Later in 2021, Vaubel et al. also reported that A-PXA show a higher number of whole chromosome CNVs than PXA grade II. Gain +7, +20, and +21 are seen to be more frequent in A-PXA. They also concluded that the majority of tumors on recurrence/anaplastic transformation acquire additional, largely nonrecurrent CNVs and a subset acquires *TERTp* mutations. In addition no tumors demonstrated concurrent gain +7/loss -10, characteristically found in GB, IDH wild type⁴⁸.

Additional mutations seen. Recently, next-generation sequencing of 295 cancer-related genes was used to investigate the molecular profiles of 13 cases of PXA by Zou et al⁵². They found that *FANCA/D2/I/M* (38%), *PRKDC* (31%), *NF1* (23%), and *NOTCH2/3/4* (23%) alterations are the most frequent somatic gene mutations in PXA after *BRAFp.V600E* (38%). There are a small number of less commonly altered genes reported in A-PXA including *ATRX*, *PTEN*, *TP53*, *BCOR*, *BCORL1*, *SPTA1*, *ARID1A*, and *BCL6*⁴⁵. Rare cases with amplification involving 8p, 12q and *PDGFRA* have also been reported^{17,50}.

Prognosis and treatment

Although PXAs are generally considered indolent neoplasms, they are associated with a higher frequency of recurrence,

malignant transformation, and death, compared with other low-grade gliomas. Studies have demonstrated that the histological WHO grade in PXA is the most significant predictor of patient OS. In a series of 62 patients the 5-year progression-free survival (PFS) and OS was 59.9% and 80.8%, respectively. This diminished with increasing grade/anaplasia with 5-year PFS and OS of 39.3% and 47.6% for A-PXA⁴⁸. In a retrospective study of 74 patients, the 5-year PFS and OS was reported to be 70.9% and 90.4% for PXA and 48.9% and 57.1% for A-PXA²¹. The frequency of recurrence of PXA has been reported to be 30% and that of malignant transformation 10–20%^{49,59,60}. Phillips et al. also demonstrated high recurrence rate in A-PXA (92%, 12/13) with a median PFS from first diagnosis of only 1.3 years (range 0.5–6.7 years)⁵⁰. Among morphological features the presence of necrosis is seen to be strongly associated with poor outcome. Five-year OS was 86.3–90.2% for tumors with no necrosis as compared to 42.2–43.8% for tumors with necrosis^{21,48}. Similarly, 5-year OS was reported to be 89.4% for tumors with mitotic activity < 5/10 HPF as compared to 55.6% for tumors with mitotic activity ≥ 5/10 HPF. Endothelial proliferation has not been reported to be associated with either OS or PFS²¹.

With regard to the age, older age at diagnosis of PXA was significantly associated with lower OS^{61,62}. However, no significant difference was reported in OS between pediatric and adult population by Ida et al, though the study found PFS to be significantly longer only in adult patients with PXA as compared to patients with A-PXA (not in pediatric patients)²¹.

Associations between patient survival and molecular alterations are less reliable due to limited number of cases in individual studies. There is still controversy with respect to the effect of *BRAFV600E* mutations and *CDKN2A/B* deletion on prognosis as various studies have reported contradictory outcomes^{15,17,21,43,63}.

TERTp mutations though rare show however strong association with shorter PFS and OS^{21,48,50}. No study has yet demonstrated any significant association of CNVs with OS^{17,50}.

Due to the rarity of the tumor standard treatment guidelines for PXA have not been established. The treatment of PXA typically involves surgical resection followed by radiological monitoring, with adjuvant treatment often utilized in patients with residual or recurrent disease following surgery or the presence of high-risk histopathological features. However, conflicting reports exist on the importance of extent of resection (EOR). Various studies found that gross total resection (GTR) conferred a significant OS advantage (10-year OS of 82%)^{10,59,64} and longer PFS as compared to subtotal resection (5 year PFS, 84.9% vs 45.4%)^{21,50}. Gianni et al. reported EOR as the single most significant predictor of recurrence-free survival in a multivariate analysis¹⁰. Contrary few studies found no difference in OS between patients who underwent GTR and those in which GTR was not achieved^{65,66}. In routine practice, GTR is feasible and safe and should be the goal of the surgeon unless for tumors extending or located over eloquent areas.

Given the paucity of data, the use of adjuvant therapy such as radiotherapy (RT) or chemotherapy (CT) is debatable. Some studies have noted an improved PFS with use of postoperative RT^{59,66–68}, but most show no benefit for the prognosis^{61,64,65}. Further, few studies demonstrated that patients who received RT in addition to surgical resection of a primary PXA tumor were at a significantly higher risk of mortality compared to those who did not receive RT. A possible explanation is that RT may induce the malignant transformation of PXA into a more aggressive tumor type with associated worse clinical outcomes⁶⁹. A case report by Hosono et al. described malignant transformation of PXA following a mutation in the *TERTp* gene after treatment with stereotactic radiosurgery⁷⁰. However, because of high recurrence rate for PXA, RT dose in the range of 45–54 Gy has been proposed by few to be considered for either adjuvant or salvage treatment. Radiation needs to be delivered using conformal techniques with image guidance to minimize long-term effects like neuro-cognitive impairment or the risk of cerebrovascular accidents. Furthermore craniospinal RT may be warranted for leptomeningeal dissemination^{67,71}.

Historically studies have variably suggested that traditional CT, such as regimes including carboplatin/VP-16, cyclophosphamide, vincristine, and temozolomide, have been minimally effective or ineffective for PXA treatment^{10,59,72,73}. Some studies documented no statistically significant relationship between OS and CT^{68,72}. The role of temozolomide (as used in infiltrative gliomas) in the management of PXA remains controversial with a general preponderance of avoiding the use of alkylating CT in the upfront adjuvant setting. Recently, a few case reports have reported that PXA with *BRAFp.V600* mutations have responded to the *BRAF* inhibitors vemurafenib or dabrafenib. Favorable responses have ranged from stable disease to complete responses^{74,75}. In the nonrandomized trial by Kaley et al. ~57% of patients with PXA treated with vemurafenib monotherapy exhibited a confirmed clinical benefit⁷⁶. Further, Thomas et al. suggested that *BRAF* inhibitors could be safely combined with antiangiogenic therapy (bevacizumab) to improve quality of life and survival in patients with disseminated A-PXA⁷³. One of the major challenges with the use of *BRAF* inhibitors remains the lack of durability of response possibly reasoned by the emergence of resistance mechanisms or activation of other driver genetic abnormalities. In the prospective trial reported by Kaley et al. of the seven patients with PXA, the median PFS was 5.7 months⁷⁶. The utilization of *BRAF* inhibitor in conjunction with tumor-treating fields has also been reported⁷⁷. Though growing experience promote the use of *BRAF* targeted therapy for treating relapsed or refractory PXAs and A-PXA, more studies are required to help elucidate the relationship between targeted CT and OS in PXA.

Other CNS tumors with histological features and/or molecular alterations similar to PXA and A-PXA

The varying morphologies within PXA conceptualize the pleomorphic nature of the tumor and may cause a diagnostic challenge from its mimics like eGB, GG, rarely GC-GB, atypical teratoid/rhabdoid tumor and heavily lipidized GB. Similarly, the molecular alterations characteristics of PXA may be noted in other CNS tumors notable being eGB, pediatric gliomas, astroblastomas (ABs) and high-grade astrocytoma with piloid (HGAP) features.

Epithelioid Glioblastoma (eGB). eGB is a rare subtype of IDH-wt GBs which was first introduced in the 2016 WHO classification of CNS tumors⁷⁸. It mostly occurs in young adults and children (median 25 years, range 3–67 years). Though eGB occurs de novo in the majority of cases, some cases have been reported to arise from lower-grade gliomas as well, most of these lower-grade lesions documented so far being PXA^{42,79,80}. In the series of 14 cases of Nakayama et al., eight cases had coexisting grade 2 or 3 diffuse glioma like lesions, one had a coexisting PXA-like component and only one had a previous history of PXA 13 years back⁴⁹. Kurshonov et al. however recognized focal areas resembling “A-PXA” in 29% (19/64) of eGB in their study⁵¹.

Studies have shown that PXAs particularly A-PXAs show significant clinical, radiological, histological and molecular overlap with eGBs resulting in difficulties when attempting to segregate these entities^{41,42}. Histological distinction of eGB appears to be more difficult from A-PXA with epithelioid morphology.

eGBs are composed of solid aggregates or loose cohesive sheets of relative uniform small to medium sized melanoma-like cells with variable “rhabdoid” features viz. abundant eosinophilic cytoplasm, eccentrically placed or centrally located vesicular nuclei, prominent nucleoli and distinct cellular membranes^{42,81}. RFs and EGBs are rare. Similarly, GCs, desmoplastic response and lipidization are less common (unlike A-PXAs). Necrosis is common but generally not palisading. Immunohistochemically eGBs are positive for OLIG2 and variably for GFAP. Immunopositivity for EMA, synaptophysin and S100 may be noted. Thus, diagnosis is often challenging, as there are no pathognomonic immunohistochemical markers, with only few small series reported till date^{81–84}.

Studies have revealed a striking similarity of molecular alterations (*BRAFp.V600E*, *TERT* promoter mutations and *CDKN2A/B* homozygous deletions) in PXAs and eGBs^{48–50}. Approximately 16.6–93% of eGBs are reported to harbor *BRAFp.V600E* mutation, which is infrequent in other types of primary GBs^{42,49,51}. Further, many studies have reported that eGBs with PXA or astrocytoma like areas show presence of *BRAF* mutation in both the components^{79,80} thus re-enforcing the fact that *BRAF* mutation might possibly be an early event to both tumors and additional genetic alterations such as *TERTp*, limbic system associated membrane protein or *CDKN2A*, is essential for malignant progression of PXA to eGB^{16,41,83}. Investigating 14 eGB, Nakajima et al. found the prevalence of *BRAFp.V600E*, *TERT* promoter mutations and *CDKN2A/B* homozygous deletions to be 93% (13/14), 71% (10/14), and 79% (11/14), respectively. Concurrent *BRAFp.V600E*, *TERT* promoter mutations and *CDKN2A/B* homozygous deletions were observed in 50% (7/14) of eGB. They also detected LOH of *ODZ3* in the eGB components of 14% (2/14) cases but not in their lower-grade components⁴⁹. Kurshonov et al. reported *BRAFp.V600E* mutation in 56% (36/64), *TERTp* mutation in 38% (24/64) and combined *BRAF/TERTp* mutations in 23% (15/64) of their eGB cases⁵¹. However, *TERTp* mutations were reported to be more frequent in the “pure” eGB (42%) vs 26% for eGB with PXA-like component⁵¹. The similarities and differences between eGB and PXA/A-PXA are summarized in Table 1.

Ganglioglioma (GG). These two tumors share the presence of EGBs, lymphocytic infiltration, immunopositivity for CD34 and *BRAFp.V600E* mutation. However, GG are less pleomorphic, and

Table 1. Similarities and differences between PXA, A-PXA and eGB.

Feature	PXA	A-PXA	eGB
Clinical features ^{10,21,41,48}			
Age, median (range), years	21 (1–85)	29 (2–79)	25 (3–67)
Pediatric	43.4%	53.1%	51.5%
Adult	56.6%	64.3%	49.5%
Location			
Supratentorial location	94.3%	100%	96%
Posterior fossa	5.7%	0	Very rare
Histomorphology ^{10,17,41–43}			
Epithelioid cells	Rare	Occasional (33.3%)	Abundant (92.3%)
Eosinophilic granular bodies	Present (83%)	Less common (13.3–66.7%)	Rare (15.4–25%)
Xanthomatous change	Present (83%)	Less common (73.3%)	Rare (25–53.8%)
Reticulin	Abundant (58%)	Less common	Rare (5%)
Intranuclear inclusion	96.7–100%	86.7%	69.2%
Lymphocytic infiltration	Present (100%)	Present (100%)	Present (100%)
Mitotic activity	Absent/low (≤ 5 /HPF)	Present (≥ 5 /HPF)	Present
Microvascular proliferation	Absent	Present/Absent	Present
Necrosis	Absent	Present/Absent (13.3%)	Present (69.2%)
Molecular features ^{17,48,50,52}			
<i>BRAFp.V600E</i> mutant	38–80%	47–64.3%	16.6–93%
<i>CDKN2A/B</i> homozygous deletion	60–>85%	78.6–93%	54.6–79%
<i>TERTp</i> mutation	4–20%	15.4–47%	38–71%
Prognosis ^{21,42}	Good	Intermediate	Worse
Median OS (months) ^{21,42}	209	51	23

have an obvious dysplastic neuronal component with no xanthomatous change (ganglion cells if encountered in PXA generally represent trapped neurons, which are morphologically normal)⁸⁵. Rarely GG can present with a glial component resembling PXA: few instances of composite tumors with features of both PXA and GG have also been reported^{85,86}. GG generally do not show homozygous deletion of *CDKN2A/B*.

Giant Cell Glioblastoma (GC-GB). They resemble PXA in that they are well circumscribed, rich in reticulin and markedly pleomorphic being composed of bizarre multinucleated GCs with frequent mitosis and necrosis. Lymphocytic infiltration may also be seen. They account for <1% of all GB with incidence of 2–5% among adult GB cases and even less in children (5–9% of pediatric GB). Mean age of presentation is 51 years (range 8–71 years) with male predominance^{87,88}. Molecularly they commonly show *TP53* mutations (80%) associated with immunopositivity for p53 protein. Mismatch repair gene defects/mutations may also be present⁸⁹. Absence of *BRAFp.V600E* mutation and presence of *MGMT* promoter hypermethylation are discriminating feature of GC-GB from PXA⁹⁰.

Atypical Teratoid/Rhabdoid Tumor (AT/RT). The distinction between PXA, eGB and AT/RT is critical in the pediatric age group. AT/RT is a malignant CNS embryonal tumor, encountered frequently in young children (median age range 16–30 months) and composed predominantly of classic rhabdoid cells admixed with variable mesenchymal, epithelial or primitive neuroectodermal components. Genetic hallmark is mutation of *SMARCB1* (*hSNF5/INI1*) gene, which lies on the long arm of chromosome 22. Approximately 0.5–2% can have *SMARCA4* gene mutation⁹¹. Lack of *INI1* immunohistochemical expression in the tumor cells is the key to diagnosis of AT/RT^{92,93}. Rare reports of AT/RT like lesion arising in PXA associated with loss of *SMARCB1* expression is available⁹⁴.

Heavily lipidized Glioblastoma. Rarely GBs can be composed predominantly of diffuse sheets of heavily lipidized, enlarged tumor cells with abundant foamy cytoplasm, thus resembling PXA. Extensive mitoses, endothelial proliferation and necrosis help in differentiating it from PXA⁹⁵.

Glioblastoma, *IDH* wild type. In a series of 302 cases, seven cases were reported to have both *BRAF* and *TERTp* mutations while only three of these seven cases had *CDKN2A/B* homozygous deletions; however, epithelioid cell morphology was not mentioned in any^{94,96,97}.

Secondary high-grade gliomas (sHGG) transforming from pediatric low-grade gliomas (PLGG). Concomitant *BRAFp.V600E* mutation and *CDKN2A/B* deletion define a distinct subgroup of pediatric LGG, which have a significantly high risk for transformation to HGG than wt PLGG. These transforming PLGG include “low-grade astrocytomas”, PAs, PXA, and GGs. Malignant transformation was observed in 2.9% of PLGGs (26/886) with prolonged latency periods for transformation (median 1.59 years vs 6.65 years for wt PLGG). The median age of diagnosis and transformation was 7 years and 12.5 years, respectively.

sHGGs exhibited a higher somatic mutation burden than primary pediatric HGGs. The most frequent alteration noted was *BRAFp.V600E* mutation and *CDKN2A* deletion observed in 39% and 57% of sHGGs, respectively. Analysis of paired cases revealed 100% and 80% concordance for *BRAF* mutations and *CDKN2A* deletion. Further, *BRAFp.V600E* was significantly more common in PLGG that transformed as compared to PLGGs that did not transform (44% vs 6%). *BRAFp.V600E* mutation was rare in primary pediatric HGGs (3%). Similarly, *CDKN2A* deletion was frequent in PLGG that transformed (71% vs 20%) as compared to PLGGs that did not transform. Concomitant *BRAFp.V600E* and *CDKN2A* deletions were seen in 75% of *BRAF* mutant PLGG. Overall, 15%

of PLGG cases that underwent malignant transformation in addition revealed *TERTp* mutation¹⁶.

Interestingly 5-year OS of children with *BRAF* mutant tumors was better (75% ± 15%) than children with wt tumors (29% ± 12%) and with primary HGG (5% ± 4%). However, after malignant transformation, 88% (23 of 26) patients died with no significant difference in survival between sHGG and primary HGG group¹⁶.

High grade astrocytoma with piloid features (HGAP). These are a new type of circumscribed astrocytic gliomas introduced in WHO 2021 Classification. They are rare tumors, which can occur throughout the neuraxis. Histologically they show a wide spectrum of features including EGBs, RFs, glomeruloid vasculature, necrosis and mitosis, thus mimicking GB, PXA and PA (especially PA with anaplastic features). Molecularly they display frequent *MAPK* pathway gene alterations [(75% (49/65)], most frequently affecting *NF1*, followed by *BRAF* (mostly *KIAA1549-BRAF* fusions) and *FGFR1* (mostly mutations) along with homozygous deletion of *CDKN2A/B* (80%, 66/83). In addition they show loss of nuclear *ATRX* expression (45%, 33/74) and are *IDH1/2* wild type. *TERTp* mutation is rare. The only method for establishing definitive diagnosis of HGAP is the distinct DNA methylation profile.

The patients have dismal prognosis, only slightly better than in *IDH*-wt GB⁹⁸. The outcome corresponds to WHO CNS grade 3 with a 5-year OS rate of ~50%. However, no definite WHO CNS grade has been yet assigned to this tumor.

Histologically defined Astroblastoma (AB)/glioma with astroblastic features. ABs are rare circumscribed glial neoplasms, presenting over a wide age range (median 44.5 years) with female predominance. They occur mostly in the cerebral hemispheres. They are characterized by predominantly perivascular papillary/pseudopapillary tumor cell arrangement, stout/thickened cell processes radiating toward the central vessels along with presence of vascular sclerosis and pericellular hyalinization. No definite histological grade is assigned to this tumor⁹⁹.

Recent studies suggested "AB" is a mere histological pattern that can be seen across a wide range of molecularly distinct tumor types. Genetic and methylation analysis have revealed that it includes several low and high-grade tumors like neuroepithelial tumors with *MN1* rearrangement, PXA-like tumors, *RELA* fusion ependymomas, and possibly few other uncharacterized lesions. However, upcoming WHO 2021 has accepted only AB with *MN1* alteration as a newly recognized tumor type, whereas the rest of molecular variants are considered contentious^{99,100}.

Lehman et al. provided evidence that ABs may be related to PXAs, based on overlapping clinicopathologic features (younger age, superficial location, presence of epithelioid/rhabdoid like cells, EGBs, multinucleated cells and perivascular lymphocytic infiltrate) and molecular features (*BRAFp.V600E* mutation and *CDKN2A* deletion). On genomic subtyping 48% of their cases ($n = 25$) grouped with high-grade neuroepithelial tumor with *MN1* alteration, 28% with PXA like and 8% with ependymoma-C11orf95-*RELA* fusion like. All the PXA-like histological ABs harbored *BRAFp.V600E* mutation with concomitant *CDKN2A/B* copy number loss in 43% *BRAF* mutant ABs¹⁰¹. In another study, 15 cases of histologically defined ABs were reclassified as either (a) PXA like (46%), (b) HGG like (33%) or (c) AB with *MN1-BEND2* fusion (6%) on genomic subtyping. PXA-like ABs harbored *BRAF* mutation with *CDKN2A* homozygous deletion in 83% and *TERT C228T* promoter mutations in 66% cases¹⁰². Similarly, Wood et al. also categorized ABs into three subtypes: (a) AB with *MN1* alteration (50%), (b) high-grade astrocytoma originally diagnosed as AB (25%) and (c) unclassifiable cases (25%)¹⁰³. The histological and molecular findings of one case from high-grade astrocytoma class were consistent with A-PXA (presence of *BRAFp.V600E* mutation, *CDKN2A* deletion and *TERTp* mutation) and was confirmed by DNA methylation grouping.

AB with molecular features of PXA and corresponding methylation pattern is frequent in adolescents and adults (31.8%) and rare in children (2.4%). Contrary, AB with *MN1* alterations is more common in children (70.7% of pediatric AB) as compared to adults (13.6%). Tumors with *MN1* rearrangement have shown significantly better outcome compared to *BRAFp.V600E*-mutant ABs^{101–104}.

Methylation profiling of PXA and A-PXA

DNA methylation profile for PXA was established by Capper et al.¹⁰⁵. It is particularly useful for tumors with ambiguous histology and is largely confirmatory for tumors with classic histology. Vaubel et al. classified 46 cases (31 PXA, 15 A-PXA) based on genome-wide methylation data and by unsupervised t-SNE, found that 40 cases grouped with PXA, 2 with anaplastic astrocytoma with piloid features, 1 with hemispheric pilocytic astrocytoma and GG, 1 with GG and 2 with control tissue. However, on histological review all the discordant cases showed characteristic histological features of PXA. Further, for the matched primary and recurrent/anaplastic-transformed samples ($n = 6$) analyzed by methylation profiling, the methylation class remained preserved⁴⁸. Therefore, though methylation profiling can largely confirm the diagnosis of PXA, it does not provide any additional information likely to alter clinical management. In addition its inability to distinguish low- and high-grade PXA represents a significant limitation of methylation-based classification.

Other tumors falling in PXA methylation group. PXA reference DNA methylation group is relatively heterogenous compared to other methylation classes and encompasses various tumors other than conventional PXAs¹⁰⁶.

Epithelioid Glioblastoma. A recent study by Kurshonov et al. documented considerable molecular and clinical heterogeneity within the eGBs by global DNA methylation and CNV analyses and established three distinct subsets: (a) PXA subset, with a high percentage of *BRAFp.V600E* mutations, but a relatively low percentage of *TERTp* mutations. In this class 34% (13/38) tumors contained PXA-like foci, 61% (23/38) showed *CDKN2A* homozygous deletions, 79% (30/38) had *BRAFp.V600E* mutations and 30% had *TERTp* mutations. These tumors occur predominantly in children and young adults and have favorable prognosis with median OS of 34 months; (b) an adult *IDH*-wt GB subset, with a relatively low percentage of *BRAFp.V600E* mutations (35%, 6/17), but a high percentage of *TERTp* mutations (83%) and *CDKN2A* homozygous deletion (53%). These tumors occur mainly in older adults and are highly aggressive, with almost all patients dying within the first 2 years (median OS 11 months) and (c) a pediatric *RTK1* subset not harboring either mutation. Cytogenetic profiles of these eGB showed enrichment for *PDGFRA* amplification (8/9; 88%), sometimes in combination with *MYCN* amplification, whereas *CDKN2A* homozygous deletions were less common (33%). This class of tumors is seen mainly in children and young adults, is associated with chromothripsis and has an intermediate prognosis (median OS 18 months). They proposed that it is likely that the "epithelioid" GB phenotype represents a mere histologic pattern rather than a variant or separate entity⁵¹.

In another series only one of four eGB had a methylation pattern that clustered with the PXAs while two other eGBs clustered with classic pediatric GB whereas a single case of epithelioid PXA clustered with methylation pattern of histologically classic PXA⁴².

Pediatric Glioblastoma/Pediatric high-grade gliomas (PHGG). Genome-wide DNA methylation recognized five subgroups among pediatric GB/PHGG ($n = 202$ and $n = 441$): H3.3 G34 mutant (15 and 11%), H3.3/H3.1 K27 mutant (43 and 27%), *IDH1* mutant (6–8%), H3/*IDH*-wt GB (35–36%) and PXA/LGG like (PXA, 9–13%

and LGG, 6%). In the group resembling PXA 48–56% (13/27 and 19/34) displayed a *BRAF*p.V600E mutation and 30% (8/27) showed homozygous 9p21 deletion, with 11% (3/27) carrying both lesions. These tumors display a favorable prognosis than those with molecular high-grade features, with 2–3-year OS of 74–91% for the LGG-like samples and 56–70% for the PXA-like tumors^{107,108}.

Relationship of PXA/A-PXA to eGB

PXAs are rare tumors having diverse morphology with potential to recur as well as disseminate throughout the CNS. Molecularly they are characterized by frequent occurrence of *MAPK* pathway alterations (with *BRAF*p.V600F mutations being most common) followed by *CDKN2A/B* deletions and *TERT*p mutations. Though described as a distinct entity in WHO, PXA shares histological, molecular as well as methylation profile features with various other tumors. One of the main reasons possibly causing the controversies regarding PXA is the ambiguity of the histological definitions. The histopathological features of PXA are variable and all of the typical characteristics are not present simultaneously nor seen in all cases. This results in considerable diagnostic challenge, of discrimination of PXA from its mimics, particularly eGB.

There are no reliable demographic, radiologic, histologic, immunohistochemical, molecular or methylation profile differences found between these PXA and eGB. There are reports of eGB developing within the tumor bed of PXA years after initial resection and cases of eGB showing a coexisting PXA component^{79,80}. It is also apparent that PXAs tend to lose the degenerative changes (EGB, reticulin fiber deposit, and intracellular xanthomatous change) with malignant transformation (Table 1), so much so that morphologically it is difficult to discriminate A-PXAs (especially epithelioid A-PXA) from eGBs due to similarity in their epithelioid pattern, increased mitosis, necrosis and lack of degenerative features. Further molecularly, PXA/A-PXA and eGB have similar genetic alterations like *TERT*p and *CDKN2A/B* deletion along with *BRAF*p.V600E mutation^{41–43}. *TERT*p mutation is thought to be involved in malignant transformation and hence its frequency increases from PXA to A-PXA and is highest in eGB (Table 1). Thus, it appears that *BRAF* mutation is an early event and additional genetic alterations of *TERT*p and *CDKN2A* are essential for malignant progression to A-PXA and development of eGB. It is also well established that a subset of eGB have methylation pattern that clusters with PXA⁵¹.

Thus based on the extensive review of literature that we have presented, we hypothesize that PXA, A-PXA and eGB are possibly a continuous histopathological and molecular spectrum—PXA being CNS WHO grade 2, A-PXA CNS WHO grade 3 and eGB CNS WHO grade 4. Thus, eGBs can either arise de novo or by malignant progression of PXA/A-PXA. The clinical outcome also supports this hypothesis with PXA having best survival, eGBs the worst (similar to other GBs) and A-PXA being intermediate.

Conclusion and future perspectives

Thus to conclude, it remains inconclusive whether PXA and eGB should be considered distinct entities, or merely a morphologic spectrum of the same entity with malignant progression, though there appears to be more evidence in support of the latter. In WHO 2021 Classification however, these two glioma types continue to be kept separate—eGB as a subtype of IDH-wt GB and PXA under “circumscribed gliomas.” Hence, more comprehensive approach for redefining these tumors incorporating histomorphology, genetic and epigenetic data should be considered in future WHO Classifications.

It is anticipated that with the evolution of molecular neuropathology, *BRAF* pathway-directed therapies will become standard treatments for *BRAF*-mutated PXA. While complete surgical resection and RT will continue to be the main components of the treatment for both PXA grade 2 and 3, novel therapeutics may

be of interest for the less responsive *BRAF* wt tumors. With regard to radiation, clinical data regarding the utility of particle therapy on reducing long-term morbidity are warranted in the future since a majority of these patients will belong to adolescent and young adult categories and are associated with excellent survival rates. The ongoing clinical trials of targeted therapeutics focused on glial tumors such as *BRAF* inhibitor (dabrafenib) in combination with *MEK* inhibitor (trametinib) (NCT02684058, NCT03919071), combinatorial targeting with *MEK* and mTOR inhibitors (PNOC021; NCT04485559), the combination of a *BRAF* inhibitor with a CDK4/6 inhibitor¹⁰⁹, a cyclin D1/CDK4/CDK6 inhibitor (ribociclib) in combination with an *MEK* inhibitor (trametinib) (NCT03434262) and intratumoral injection of an oncolytic recombinant polio virus/rhinovirus (PVSRIPO) (NCT03043391) may help confirm new therapeutic targets for PXAs.

REFERENCES

- Kepes, J. J., Rubinstein, L. J. & Eng, L. F. Pleomorphic xanthoastrocytoma: a distinctive meningocerebral glioma of young subjects with relatively favorable prognosis. A study of 12 cases. *Cancer* **44**, 1839–1852 (1979).
- Weldon-Linne, C. M., Victor, T. A., Groothuis, D. R. & Vick, N. A. Pleomorphic xanthoastrocytoma. Ultrastructural and immunohistochemical study of a case with a rapidly fatal outcome following surgery. *Cancer* **52**, 2055–2063 (1983).
- Iwaki, T., Fukui, M., Kondo, A., Matsushima, T. & Takeshita, I. Epithelial properties of pleomorphic xanthoastrocytomas determined in ultrastructural and immunohistochemical studies. *Acta Neuropathol.* **74**, 142–150 (1987).
- Kepes, J. J., Rubinstein, L. J., Ansbacher, L. & Schreiber, D. J. Histopathological features of recurrent pleomorphic xanthoastrocytomas: further corroboration of the glial nature of this neoplasm. A study of 3 cases. *Acta Neuropathol.* **78**, 585–593 (1989).
- Kleihues, P., Burger, P. C. & Scheithauer, B. W. The new WHO classification of brain tumours. *Brain Pathol.* **3**, 255–268 (1993).
- Kleihues, P. et al. The WHO classification of tumors of the nervous system. *J. Neuropathol. Exp. Neurol.* **61**, 215–225 (2002).
- Louis, D. N. et al. The 2007 WHO classification of tumours of the central nervous system. *Acta Neuropathol.* **114**, 97–109 (2007).
- Okazaki, T. et al. Primary anaplastic pleomorphic xanthoastrocytoma with widespread neuroaxis dissemination at diagnosis—a pediatric case report and review of the literature. *J. Neurooncol.* **94**, 431–437 (2009).
- Kyritsis, A. P. et al. Mutations of the p16 gene in gliomas. *Oncogene* **12**, 63–67 (1996).
- Giannini, C. et al. Pleomorphic xanthoastrocytoma: what do we really know about it? *Cancer* **85**, 2033–2045 (1999).
- Giannini, C., et al. Anaplastic pleomorphic xanthoastrocytoma. in *WHO Classification of Tumours of the Central Nervous System* (eds Louis, D. N., Ohgaki, H., Wiestler, O. D., Cavenee, W. K.) 4th edn, 98–99 (IARC, 2016).
- Dias-Santagata, D. et al. *BRAF* V600E mutations are common in pleomorphic xanthoastrocytoma: diagnostic and therapeutic implications. *PLoS ONE* **6**, e17948 (2011).
- Schindler, G. et al. Analysis of *BRAF* V600E mutation in 1,320 nervous system tumors reveals high mutation frequencies in pleomorphic xanthoastrocytoma, ganglioglioma and extra-cerebellar pilocytic astrocytoma. *Acta Neuropathol.* **121**, 397–405 (2011).
- Weber, R. G. et al. Frequent loss of chromosome 9, homozygous *CDKN2A/p14* (ARF)/*CDKN2B* deletion and low *TSC1* mRNA expression in pleomorphic xanthoastrocytomas. *Oncogene* **26**, 1088–1097 (2007).
- Lassaletta, A. et al. Therapeutic and prognostic implications of *BRAF* V600E in pediatric low-grade gliomas. *J. Clin. Oncol.* **35**, 2934–2941 (2017).
- Mistry, M. et al. *BRAF* mutation and *CDKN2A* deletion define a clinically distinct subgroup of childhood secondary high-grade glioma. *J. Clin. Oncol.* **33**, 1015–1022 (2015).
- Vaubel, R. A. et al. Recurrent copy number alterations in low-grade and anaplastic pleomorphic xanthoastrocytoma with and without *BRAF* V600E mutation. *Brain Pathol.* **28**, 172–182 (2018).
- Giannini, C. et al. Pleomorphic xanthoastrocytoma. in *The WHO Classification of Tumors of the Central Nervous System* (eds Reifenberger, G. & Perry, A.) 5th edn (IARC) (2007).
- Dono, A. et al. Predictors of outcome in pleomorphic xanthoastrocytoma. *Neurooncol. Pract.* **8**, 222–229 (2020).
- Ostrom, Q. T. et al. CBTRUS statistical report: primary brain and other central nervous system tumors diagnosed in the United States in 2010–2014. *Neuro Oncol.* **19**, v1–v88 (2017).

21. Ida, C. M. et al. Pleomorphic xanthoastrocytoma: natural history and long-term follow-up. *Brain Pathol.* **25**, 575–586 (2015).
22. Dolecek, T. A., Propp, J. M., Stroup, N. E. & Kruchko, C. CBTRUS statistical report: primary brain and central nervous system tumors diagnosed in the United States in 2005–2009. *Neuro Oncol.* **14**(Suppl 5), v1–v49 (2012).
23. Fouladi, M. et al. Pleomorphic xanthoastrocytoma: favorable outcome after complete surgical resection. *Neuro Oncol.* **3**, 184–192 (2001).
24. Gil-Gouveia, R. et al. Pleomorphic xanthoastrocytoma of the cerebellum: illustrated review. *Acta Neurochir.* **146**, 1241–1244 (2004).
25. Nakamura, M., Chiba, K., Matsumoto, M., Ikeda, E. & Toyama, Y. Pleomorphic xanthoastrocytoma of the spinal cord. Case report. *J. Neurosurg. Spine* **5**, 72–75 (2006).
26. Zarate, J. O. & Sampaolesi, R. Pleomorphic xanthoastrocytoma of the retina. *Am. J. Surg. Pathol.* **23**, 79–81 (1999).
27. McNatt, S. A., Gonzalez-Gomez, I., Nelson, M. D. & McComb, J. G. Synchronous multicentric pleomorphic xanthoastrocytoma: case report. *Neurosurgery* **57**, E191 (2005).
28. Lubansu, A. et al. Cerebral anaplastic pleomorphic xanthoastrocytoma with meningeal dissemination at first presentation. *Childs Nerv. Syst.* **20**, 119–122 (2004).
29. Passone, E. et al. Non-anaplastic pleomorphic xanthoastrocytoma with neuro-radiological evidences of leptomeningeal dissemination. *Childs Nerv. Syst.* **22**, 614–618 (2006).
30. Davies, K. G., Maxwell, R. E., Seljeskog, E. & Sung, J. H. Pleomorphic xanthoastrocytoma-report of four cases, with MRI scan appearances and literature review. *Br. J. Neurosurg.* **8**, 681–689 (1994).
31. Crespo-Rodriguez, A. M., Smirniotopoulos, J. G. & Rushing, E. J. MR and CT imaging of 24 pleomorphic xanthoastrocytomas (PXA) and a review of the literature. *Neuroradiology* **49**, 307–315 (2007).
32. Osborn A. G., Blaser S. I. & Salzman K. L. (eds) *Diagnostic Imaging: Brain* 1st edn (Amirsys, 2004).
33. Yu, S., He, L., Zhuang, X. & Luo, B. Pleomorphic xanthoastrocytoma: MR imaging findings in 19 patients. *Acta Radiol.* **52**, 223–228 (2011).
34. Yoshino, M. T. & Lucio, R. Pleomorphic xanthoastrocytoma. *Am. J. Neuroradiol.* **13**, 1330–1332 (1992).
35. Bucciero, A. et al. Pleomorphic xanthoastrocytoma: clinical, imaging and pathological features of four cases. *Clin. Neurol. Neurosurg.* **99**, 40–45 (1997).
36. Kepes, J. J., Kepes, M. & Slowik, F. Fibrous xanthomas and xanthosarcomas of the meninges and the brain. *Acta Neuropathol.* **23**, 187–199 (1973).
37. Burger P. C. & Scheithauer B. W. *Tumors of the Central Nervous System* (American Registry of Pathology in collaboration with the Armed Forces Institute of Pathology, 2007).
38. Perry A. & Brat D. J. *Practical Surgical Neuropathology: a Diagnostic Approach* (Elsevier, 2018).
39. Primavera, J. et al. Clear cell pleomorphic xanthoastrocytoma: case report. *Acta Neuropathol.* **102**, 404–408 (2001).
40. Xiong, J., Chu, S. G., Mao, Y. & Wang, Y. Pigmented pleomorphic xanthoastrocytoma: a rare variant and literature review. *Neuropathology* **31**, 88–92 (2011).
41. Furuta, T. et al. Clinicopathological and genetic association between epithelioid glioblastoma and pleomorphic xanthoastrocytoma. *Neuropathology* **38**, 218–227 (2018).
42. Alexandrescu, S. et al. Epithelioid glioblastomas and anaplastic epithelioid pleomorphic xanthoastrocytomas-same entity or first cousins? *Brain Pathol.* **26**, 215–223 (2016).
43. Wang, J. et al. Evaluation of EZH2 expression, BRAF V600E mutation, and CDKN2A/B deletions in epithelioid glioblastoma and anaplastic pleomorphic xanthoastrocytoma. *J. Neurooncol.* **144**, 137–146 (2019).
44. Hirose, T. et al. Pleomorphic xanthoastrocytoma: a comparative pathological study between conventional and anaplastic types. *Histopathology* **52**, 183–193 (2008).
45. Giannini, C., Hebrink, D., Scheithauer, B. W., Dei Tos, A. P. & James, C. D. Analysis of p53 mutation and expression in pleomorphic xanthoastrocytoma. *Neurogenetics* **3**, 159–162 (2001).
46. Paulus, W. et al. Molecular genetic alterations in pleomorphic xanthoastrocytoma. *Acta Neuropathol.* **91**, 293–297 (1996).
47. Kaulich, K. et al. Genetic alterations commonly found in diffusely infiltrating cerebral gliomas are rare or absent in pleomorphic xanthoastrocytomas. *J. Neuropathol. Exp. Neurol.* **61**, 1092–1099 (2002).
48. Vaubel, R. et al. Biology and grading of pleomorphic xanthoastrocytoma-what have we learned about it? *Brain Pathol.* **31**, 20–32 (2021).
49. Nakajima, N. et al. BRAF V600E, TERT promoter mutations and CDKN2A/B homozygous deletions are frequent in epithelioid glioblastomas: a histological and molecular analysis focusing on intratumoral heterogeneity. *Brain Pathol.* **28**, 663–673 (2018).
50. Phillips, J. J. et al. The genetic landscape of anaplastic pleomorphic xanthoastrocytoma. *Brain Pathol.* **29**, 85–96 (2019).
51. Korshunov, A. et al. Epithelioid glioblastomas stratify into established diagnostic subsets upon integrated molecular analysis. *Brain Pathol.* **28**, 656–662 (2018).
52. Zou, H. et al. Molecular features of pleomorphic xanthoastrocytoma. *Hum. Pathol.* **86**, 38–48 (2019).
53. Koelsche, C. et al. Distribution of TERT promoter mutations in pediatric and adult tumors of the nervous system. *Acta Neuropathol.* **126**, 907–915 (2013).
54. Pratt, D. et al. BRAF activating mutations involving the β 3- α C loop in V600E-negative anaplastic pleomorphic xanthoastrocytoma. *Acta Neuropathol. Commun.* **6**, 24 (2018).
55. Hsiao, S. J. et al. A novel, potentially targetable TMEM106B-BRAF fusion in pleomorphic xanthoastrocytoma. *Cold Spring Harb. Mol. Case Stud.* **3**, a001396 (2017).
56. Zhang, J. St. Jude Children’s Research Hospital–Washington University Pediatric Cancer Genome Project. et al. Whole-genome sequencing identifies genetic alterations in pediatric low-grade gliomas. *Nat. Genet.* **45**, 602–612 (2013).
57. Bettegowda, C. et al. Exomic sequencing of four rare central nervous system tumor types. *Oncotarget* **4**, 572–583 (2013).
58. Phillips, J. J. et al. Activating NRF1-BRAF and ATG7-RAF1 fusions in anaplastic pleomorphic xanthoastrocytoma without BRAF p.V600E mutation. *Acta Neuropathol.* **132**, 757–760 (2016).
59. Lim, S. et al. Prognostic factors and therapeutic outcomes in 22 patients with pleomorphic xanthoastrocytoma. *J. Korean Neurosurg. Soc.* **53**, 281–287 (2013).
60. Korshunov, A. & Golanov, A. Pleomorphic xanthoastrocytomas: immunohistochemistry, grading and clinico-pathologic correlations. An analysis of 34 cases from a single Institute. *J. Neurooncol.* **52**, 63–72 (2001).
61. Perkins, S. M., Mitra, N., Fei, W. & Shinohara, E. T. Patterns of care and outcomes of patients with pleomorphic xanthoastrocytoma: a SEER analysis. *J. Neurooncol.* **110**, 99–104 (2012).
62. Ng, W. H., Lim, T. & Yeo, T. T. Pleomorphic xanthoastrocytoma in elderly patients may portend a poor prognosis. *J. Clin. Neurosci.* **15**, 476–478 (2008).
63. Reis, G. F. et al. CDKN2A loss is associated with shortened overall survival in lower-grade (World Health Organization Grades II–III) astrocytomas. *J. Neuro-pathol. Exp. Neurol.* **74**, 442–452 (2015).
64. Pahapill, P. A., Ramsay, D. A. & Del Maestro, R. F. Pleomorphic xanthoastrocytoma: case report and analysis of the literature concerning the efficacy of resection and the significance of necrosis. *Neurosurgery* **38**, 822–829 (1996).
65. Byun, J., Hong, S. H., Kim, Y.-H., Kim, J. H. & Kim, C. J. Peritumoral edema affects the prognosis in adult pleomorphic xanthoastrocytoma: retrospective analysis of 25 patients. *World Neurosurg.* **114**, e457–e467 (2018).
66. Macaulay, R. J., Jay, V., Hoffman, H. J. & Becker, L. E. Increased mitotic activity as a negative prognostic indicator in pleomorphic xanthoastrocytoma: case report. *J. Neurosurg.* **79**, 761–768 (1993).
67. Koga, T. et al. Long-term control of disseminated pleomorphic xanthoastrocytoma with anaplastic features by means of stereotactic irradiation. *Neuro Oncol.* **11**, 446–451 (2009).
68. van Roost, D., Kristof, R., Zentner, J., Wolf, H. K. & Schramm, J. Clinical, radiological, and therapeutic features of pleomorphic xanthoastrocytoma: report of three patients and review of the literature. *J. Neurol. Neurosurg. Psychiatry* **60**, 690–692 (1996).
69. Khalafallah, A., Rakovec, M. & Mukherjee, D. Association between adjuvant radiation therapy and overall survival in pleomorphic xanthoastrocytoma. *Clin. Neurol. Neurosurg.* **196**, 106042 (2020).
70. Hosona, J. et al. Role of a promoter mutation in TERT in malignant transformation of pleomorphic xanthoastrocytoma. *World Neurosurg.* **126**, 624–630 (2019).
71. Saikali, S. et al. Multicentric pleomorphic xanthoastrocytoma in a patient with neurofibromatosis type 1: case report and review of the literature. *J. Neurosurg.* **102**, 376–381 (2005).
72. Mallick, S., Benson, R., Melgandhi, W., Giridhar, P. & Rath, G. K. Grade II pleomorphic xanthoastrocytoma: a meta-analysis of data from previously reported 167 cases. *J. Clin. Neurosci.* **54**, 57–62 (2018).
73. Thomas, A. et al. RARE-30. Anaplastic pleomorphic xanthoastrocytoma with leptomeningeal dissemination responsive to BRAF inhibition and bevacizumab. *Neuro Oncol.* **19**, vi216 (2017). Suppl. 6.
74. Brown, N. F., Carter, T. & Mulholland, P. Dabrafenib in BRAFV600-mutated anaplastic pleomorphic xanthoastrocytoma. *CNS Oncol.* **6**, 5–9 (2017).
75. Hyman, D. M. et al. Vemurafenib in multiple nonmelanoma cancers with BRAF V600 mutations. *N. Engl. J. Med.* **373**, 726–736 (2015).
76. Kaley, T. et al. BRAF inhibition in BRAF^{V600}-mutant gliomas: results from the VEBASKET Study. *J. Clin. Oncol.* **36**, 3477–3484 (2018).
77. Lukas, R. V. & Merrell, R. T. BRAF inhibition with concomitant tumor treating fields for a multiply progressive pleomorphic xanthoastrocytoma. *CNS Oncol.* **7**, CNS10 (2018).

78. Louis, D. N. et al. The 2016 World Health Organization Classification of Tumors of the Central Nervous System: a summary. *Acta Neuropathol.* **131**, 803–820 (2016).
79. Tanaka, S. et al. Epithelioid glioblastoma arising from pleomorphic xanthoastrocytoma with the BRAF V600E mutation. *Brain Tumor Pathol.* **31**, 172–176 (2014).
80. Matsumura, N. et al. Concurrent TERT promoter and BRAF V600E mutation in epithelioid glioblastoma and concomitant low-grade astrocytoma. *Neuropathology* **37**, 58–63 (2017).
81. Broniscer, A. et al. Clinical, radiological, histological and molecular characteristics of paediatric epithelioid glioblastoma. *Neuropathol. Appl. Neurobiol.* **40**, 327–336 (2014).
82. Kleinschmidt-DeMasters, B. K. et al. Epithelioid versus rhabdoid glioblastomas are distinguished by monosomy 22 and immunohistochemical expression of INI-1 but not claudin 6. *Am. J. Surg. Pathol.* **34**, 341–354 (2010).
83. Nobusawa, S. et al. Intratumoral heterogeneity of genomic imbalance in a case of epithelioid glioblastoma with BRAF V600E mutation. *Brain Pathol.* **24**, 239–246 (2014).
84. Khanna, G. et al. Immunohistochemical and molecular genetic study on epithelioid glioblastoma: series of seven cases with review of literature. *Pathol. Res. Pract.* **214**, 679–685 (2018).
85. Kordek, R. et al. Pleomorphic xanthoastrocytoma with a gangliomatous component: an immunohistochemical and ultrastructural study. *Acta Neuropathol.* **89**, 194–197 (1995).
86. Perry, A. et al. Composite pleomorphic xanthoastrocytoma and ganglioglioma: report of four cases and review of the literature. *Am. J. Surg. Pathol.* **21**, 763–771 (1997).
87. Margetts, J. C. & Kalyan-Raman, U. P. Giant celled glioblastoma of brain: a clinico-pathological and radiological study of ten cases (including immunohistochemistry and ultrastructure). *Cancer* **63**, 524–531 (1989).
88. Kozak, K. R. & Moody, J. S. Giant cell glioblastoma: a glioblastoma subtype with distinct epidemiology and superior prognosis. *Neuro Oncol.* **11**, 833–841 (2009).
89. Meyer-Puttitz, B. et al. Molecular genetic analysis of giant cell glioblastomas. *Am. J. Pathol.* **151**, 853–857 (1997).
90. Ogawa, K. et al. Giant cell glioblastoma is a distinctive subtype of glioma characterized by vulnerability to DNA damage. *Brain Tumor Pathol.* **37**, 5–13 (2020).
91. Nesvick, C. L. et al. Atypical teratoid rhabdoid tumor: molecular insights and translation to novel therapeutics. *J. Neurooncol.* **150**, 47–56 (2020).
92. Ho, B. et al. Molecular subgrouping of atypical teratoid/rhabdoid tumors—a reinvestigation and current consensus. *Neuro Oncol.* **22**, 613–624 (2020).
93. Uner, M., Saglam, A., Meydan, B. C., Aslan, K. & Soylemezoglu, F. Atypical teratoid rhabdoid tumor arising in a pleomorphic xanthoastrocytoma: a rare entity. *Clinic Neuropathol.* **36**, 227–232 (2017).
94. Zacher, A. et al. Molecular diagnostics of gliomas using next generation sequencing of a glioma-tailored gene panel. *Brain Pathol.* **27**, 146–159 (2017).
95. Gupta, K., Kalra, I., Salunke, P. & Vasishta, R. K. Lipidized glioblastoma: a rare differentiation pattern. *Neuropathology* **31**, 93–97 (2011).
96. Arita, H. et al. A combination of TERT promoter mutation and MGMT methylation status predicts clinically relevant subgroups of newly diagnosed glioblastomas. *Acta Neuropathol. Commun.* **4**, 79 (2016).
97. Ceccarelli, M. et al. Molecular profiling reveals biologically discrete subsets and pathways of progression in diffuse glioma. *Cell* **164**, 550–563 (2016).
98. Reinhardt, A. et al. Anaplastic astrocytoma with piloid features, a novel molecular class of IDH wildtype glioma with recurrent MAPK pathway, CDKN2A/B and ATRX alterations. *Acta Neuropathol.* **136**, 273–291 (2018).
99. Aldape K. D. & Rosenblum M. K. Astroblastoma. in *WHO Classification of Tumours of the Central Nervous System* (Louis, D. N., Ohgaki, H., Wiestler, O. D. & Cavenee, W. K.) 121–122 (International Agency for Research on Cancer, 2016).
100. Lehman, N. L. et al. Genomic analysis demonstrates that histologically-defined astroblastomas are molecularly heterogeneous and that tumors with MN1 rearrangement exhibit the most favorable prognosis. *Acta Neuropathol. Commun.* **7**, 42 (2019).
101. Lehman, N. L. et al. Morphological and molecular features of astroblastoma, including BRAFV600E mutations, suggest an ontological relationship to other cortical-based gliomas of children and young adults. *Neuro-Oncology* **19**, 31–42 (2017).
102. Boisseau, W. et al. Molecular profiling reclassifies adult astroblastoma into known and clinically distinct tumor entities with frequent mitogen-activated protein kinase pathway alterations. *Oncologist* **24**, 1584–1592 (2019).
103. Wood, M. D. et al. Multimodal molecular analysis of astroblastoma enables reclassification of most cases into more specific molecular entities. *Brain Pathol.* **28**, 192–202 (2018).
104. Sturm, D. et al. New brain tumor entities emerge from molecular classification of CNS-PNETs. *Cell* **164**, 1060–1072 (2016).
105. Capper, D. et al. DNA methylation-based classification of central nervous system tumours. *Nature* **555**, 469–474 (2018).
106. Fukuoka, K. et al. Clinical impact of combined epigenetic and molecular analysis of pediatric low-grade gliomas. *Neuro Oncol.* **22**, 1474–1483 (2020).
107. Korshunov, A. et al. Integrated analysis of pediatric glioblastoma reveals a subset of biologically favorable tumors with associated molecular prognostic markers. *Acta Neuropathol.* **129**, 669–678 (2015).
108. Mackay, A. et al. Integrated molecular meta-analysis of 1,000 pediatric high-grade and diffuse intrinsic pontine glioma. *Cancer Cell* **32**, 520–537 (2017).
109. Huillard, E. et al. Cooperative interactions of BRAFV600E kinase and CDKN2A locus deficiency in pediatric malignant astrocytoma as a basis for rational therapy. *Proc. Natl Acad. Sci. USA* **109**, 8710–8715 (2012).

ACKNOWLEDGEMENTS

The authors wish to acknowledge Dr. Tejpal Gupta, Professor and Officer in charge, Department of Radiation Oncology, Tata Memorial Centre, Mumbai, India, for his inputs and edits in the treatment section of this review.

AUTHOR CONTRIBUTIONS

SM and CS: conceptualization, data curation, writing and editing. VS, ID and MCS: data curation.

COMPETING INTERESTS

The authors declare no competing interests.

ADDITIONAL INFORMATION

Correspondence and requests for materials should be addressed to Vaishali Suri or Chitra Sarkar.

Reprints and permission information is available at <http://www.nature.com/reprints>

Publisher's note Springer Nature remains neutral with regard to jurisdictional claims in published maps and institutional affiliations.